

Determination of parameters for a half-band filter in a digital Hilbert transformer in a reactive power measurement system

Abstract. This article presents a selection analysis of the parameters used for a half-band filter in a digital Hilbert transformer. The parameters were determined for the transformer's use in measuring Budeanu reactive power. This solution allowed to check the operation of the filter by comparing the results obtained with the filter with the results of Budeanu reactive power obtained in the frequency domain. Fifty half-band filters were designed and tested. As a result of the analysis the best filter was chosen. For this half-band filter the obtained values of the relative error of the reactive power measurement were less than or equal to 0.01% for different types of load parameters, signals and sampling frequencies.

Streszczenie. W artykule przedstawiono analizę doboru parametrów filtra half-band, stosowanego w transformatorze Hilberta. Parametry te określono dla transformatora zastosowanego do pomiaru mocy biernej według Budeanu. Rozwiązanie takie pozwoliło sprawdzić działanie filtra porównując otrzymane z jego użyciem wyniki mocy z wynikami otrzymanymi w dziedzinie częstotliwości ze wzoru Budeanu. Do testów zaprojektowano pięćdziesiąt filtrów Hilberta. Z nich wybrano filtr o najlepszych parametrach, dla których błąd pomiaru mocy biernej był mniejszy lub równy 0.01% dla różnych sygnałów wejściowych, typów odbiornika i częstotliwości próbkowania. (Dobór parametrów filtra half-band dla cyfrowego transformatora Hilberta w układzie do pomiaru mocy biernej).

Keywords: half-band filter, Hilbert transformer, reactive power measurement.

Słowa kluczowe: filtr half-band, transformator Hilberta, pomiar mocy biernej.

Introduction

The Hilbert transform converts an input real signal into a different real signal, shifted by phase about -90 degrees for $0 \leq \omega < \pi$, and about 90 deg for $-\pi \leq \omega < 0$ in relation to the input signal [1, 2]. All input signal frequency components are shifted. The Hilbert transformer, which makes the actual Hilbert transform, can operate in the frequency domain or in the time domain. In the second case, the ideal Hilbert transformer is a filter or a system of filters, whose frequency response $H(j\omega)$ is given by

$$(1) \quad H(j\omega) = \begin{cases} -j, & \omega > 0 \\ 0, & \omega = 0 \\ j, & \omega < 0 \end{cases}$$

and the magnitude response by $|H(j\omega)| = 1$ [2].

A Hilbert transformer can be used, amongst other things, for measurement of reactive power in the time domain according to the equation defined by Nowomiejski [3, 4], which is described as follows:

$$(2) \quad Q = \frac{1}{kT} \int_{\tau}^{\tau+kT} u(t)H[i(t)]dt = \frac{-1}{kT} \int_{\tau}^{\tau+kT} i(t)H[u(t)]dt$$

where: $H[u(t)]$, $H[i(t)]$ – the voltage and current Hilbert transforms.

Equation (2) gives the same results as for Budeanu reactive power [4, 5] described in the formula

$$(3) \quad Q = \sum_{i=1}^{\infty} U_i I_i \sin \varphi_i = \sum_{i=1}^{\infty} Q_i$$

where: U_i is the rms value of the voltage harmonic, I_i is the rms value of the current harmonic, φ_i is the phase angle between the current and the voltage harmonics.

It can therefore be assumed that formula (2) expresses Budeanu reactive power in the time domain.

This article presents an analysis of a selection of parameters for a half-band filter used in a digital Hilbert transformer. The parameters were determined for the transformer's use in measuring Budeanu reactive power in the time domain, although at present reactive power is determined from the definition of Iliovici [6, 7]. The aim here

is the later development of a measurement system with a phase shifter, with additional correction to convert the results of Budeanu reactive power obtained in the time domain into results obtainable by performing measurements according to Iliovici's definition. Work on such a system is underway by the author and other researchers [8].

Hilbert transformer

A Hilbert transformer can be realised using discrete finite impulse response filters (FIR) or infinite impulse response filters IIR [1, 2]. A different, interesting way to realise the Hilbert transformer in domain time, is to use a phase splitter [9, 10, 11]. This works as a system including two all-pass filters F_1 and F_2 (Fig. 1), which phase characteristics differ from each other by ca. -90 degrees. The system does not create a signal directly equal to the Hilbert transform of the input signal, but gives two output signals, which are the mutual Hilbert transforms of each other.

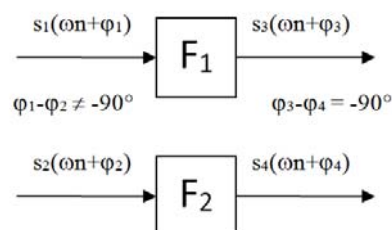


Fig. 1. Phase splitter.

The amplitude frequency characteristics of the filters F_1 and F_2 should satisfy $|H_1(e^{j\omega})| = |H_2(e^{j\omega})| = 1$ in the frequency range $(\omega_0, \pi - \omega_0)$, where $H_1(e^{j\omega})$ and $H_2(e^{j\omega})$ are the transfer functions of F_1 and F_2 . The transfer functions should satisfy the equation for the Hilbert phase-shift characteristic [10]:

$$(4) \quad \frac{H_1(e^{j\omega})}{H_2(e^{j\omega})} = -j, \quad \omega_0 < \omega < \pi - \omega_0$$

The all-pass filters can be realised as a cascade of the low-order all-pass sections. A design method for IIR Hilbert all-pass filters based on half-band filtering was presented by Rashid [12, 13]. In this method, the half-band filter is obtained by modifying the conventional elliptic filters, so that

all the poles of the half-band filter lie on an imaginary axis [12]. The transfer function of the half-band IIR filter [12] can then be written as

$$(5) \quad H_{HB}(z) = z^{-1}H_{F0}(z^2) + H_{F2}(z^2)$$

where $H_{F0}(z^2)$ and $H_{F2}(z^2)$ are the all-pass filters.

The half-band filter has the frequency range $(-\omega_p, \omega_p)$ [14], where $\omega_p < \pi/2$ is the circular passband edge frequency. For the purpose of obtaining the band frequency $\omega_0 < \omega < \pi - \omega_0$, ($\omega_0 > 0$), it is necessary to perform a frequency shift by $\pi/2$. The shift is achieved by substituting z for $-jz$ into (5), which yields $z^{-1}H_{F0}(-z^2)$ and $H_{F2}(-z^2)$ [11, 13]. The last transfer will constitute a pair of 90 degree phase shifters. After the mathematical transformations, we obtain the transfer functions of two digital all-pass filters H_{F1} (6) and H_{F2} (7) [10], which can then be implemented in digital signal processing (DSP) systems.

$$(6) \quad H_{F1}(z) = z^{-1} \prod_{a_i > 1} \frac{1 - z^{-2}}{1 - \frac{1}{a_i} z^{-2}}$$

$$(7) \quad H_{F2}(z) = \prod_{a_i \leq 1} \frac{a_i - z^{-2}}{1 - a_i z^{-2}}$$

The procedure for calculating the coefficients a_i is described in literature [12, 15]. The computer algorithm used to calculate the filter coefficients is presented in [15]. To make the calculations, the following parameters of the half-band filter have to be brought in to the algorithm: the passband edge (ω_p) in units of π , and the ripples of the passband and the stop-band (δ_p and δ_s) [14, 15]. The actual cut-off frequency ω_0 of the designed Hilbert transform may be different than the frequency $\pi/2 - \omega_p$. But it does satisfy the formula $\omega_0 \leq \pi/2 - \omega_p$ [16], and depends on the half-band filter parameters used. The usefulness of the half-band filter in reactive power measurement also depends on its parameters. The results obtained from simulations show that small changes of the filter's parameters' values can cause very large errors in reactive power measurement. Therefore, it is essential to select the proper filter parameters. In order to choose the best set of coefficients, the Author performed a comparative analysis of 50 half-band filters with different parameters' values, which are described in the next point.

Model of the measurement system

A model of the reactive power measurement system was made in Matlab with Simulink and Power System Blockset Toolboxes (Fig. 2). It consisted of a deformed voltage source, an RLC load, blocks to measure the instantaneous current and voltage values, analog-to-digital converters and systems for recording signals.

Calculation of the reactive power using a fast Fourier transform (FFT) and the Hilbert transformer were made in Matlab. Suitable DSP algorithms were implemented in M-files. The code for the calculation of the reactive power using equation (3), on the basis of 50 voltage and current harmonics, and the formula

$$(8) \quad Q = \frac{1}{N} \sum_{n=0}^{N-1} i_{F2}(n) u_{F1}(n)$$

where: i_{F2} is the discrete current signal received by filtering of the load current signal by means of the all-pass filter H_{F2} (7), and u_{F1} is the discrete voltage signal received by

filtering of the load voltage signal through the all-pass filter H_{F1} (6).

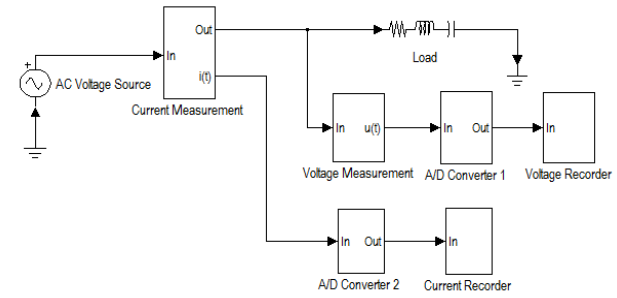


Fig. 2. Diagram of the model of the measurement system.

The coefficients for the filters H_{F1} and H_{F2} were calculated for the half-band filter parameters, given in Table 1. Six sets of the filters were designed for each specified circular frequency ω_p . Each set of half-band filters was designed with the same values for δ_p and δ_s , which are equal to $1e-2$, $1e-3$, $1e-4$, $1e-5$, $1e-6$ and $1e-7$ respectively (for simplicity's sake, in the following text $\delta_p = \delta_s = d$).

Table 1. Half-band filter parameters used to calculate their coefficients.

Designation of the filters characteristics given in Figures 3-11	Low cut-off frequency f_0 of the Hilbert transformer passband (related to the circular frequency ω_0) [Hz]	Cut-off frequency of the half-band filter $f_p = f_s/4 - f_0$ where f_s - the sampling frequency [Hz]	Passband edge circular frequency ω_p of the half-band filter [π]
1	5	3195	0.49922
2	10	3190	0.49844
3	20	3180	0.49688
4	30	3170	0.49531
5	40	3160	0.49375
6	50	3150	0.49219
7	60	3140	0.49063
8	100	3100	0.48438

Additionally, two half-band filters were designed for d equal to $1e-5$ and f_0 equal to 5.2 Hz and 5.5 Hz, the necessity of which arose during the simulation. In total, 50 half-band filters were designed, but because of the limited page count of this article, only the coefficients for the best half-band filter, which gives the most accurate values of the reactive power (chosen during the simulation tests) are presented. Low cut-off frequencies f_0 greater than 50 Hz were also used in the model, which was designed to examine how shifting of the frequency band of the Hilbert transformer influences real processing characteristics and measurement results. In practice, it is possible that the real frequency bands of the half-band filters may be shifted due to low accuracy of the electronic elements, or the limited capabilities of the equipment used. Two voltage signals generated in the model were used for testing, with the first used to examine all of the designed Hilbert transforms. It consisted of five odd harmonics and is described by

$$(9) \quad u_{s1}(t) = \sum_{k=1}^9 U_k \sin(2\pi f_k t)$$

where: $k = 1, 3 \dots 9$, $f_1 = 50$ Hz, $U_1 = 325.27$ V, $U_3 = 32.527$ V, $U_5 = 16.2635$ V, $U_7 = 6.5054$ V, $U_9 = 3.2557$ V

The second signal consisted of eleven odd harmonics and is described by

$$(10) \quad u_{s2}(t) = \sum_{k=1}^{21} U_k \sin(2\pi f_k t)$$

where: $k = 1, 3 \dots 21$, $f_1 = 50$ Hz, $U_1 = 325.27$ V, $U_3 = 65.054$ V, $U_5 = 48.7905$ V, $U_{7,9,11,13,15,17,19,21} = 32.527$ V

This signal was used to test five filters chosen during the first selection. Measurements were made for resistive (R), resistive-inductive (RL) and resistive-capacitive (RC) loads. In all cases, the passive elements were connected in series. Tests with signal u_{s1} were run for five sets of load parameters. Tests with signal u_{s2} were run for eight resistive-inductive and six resistive-capacitive loads. All load parameters are given in Table 2.

Table 2. The load parameters used for signals u_{s1} and u_{s2} .

No.	Set for u_{s1}		Set for u_{s1}		Set for u_{s2}		Set for u_{s2}	
	R [Ω]	L [mH]	R [Ω]	C [mF]	R [Ω]	L [mH]	R [Ω]	C [mF]
1	10		10	2	10	0.1	10	0.01
2	10	100	10	60	10	0.5	10	0.6
3	10	0.1			10	1	10	1
4					10	5	10	6
5					10	10	10	10
6					10	50	10	60
7					10	100		
8					10	500		

Load parameter values were made experimentally. In the model, calculations of the reactive power were also made in the frequency domain on the basis of 50 voltage and current harmonics, in every input signal period. This required processing of the signals in a frequency band from 0 Hz to 2.5 kHz. The minimum sampling frequency that satisfies the sampling theorem and enables collection of 2n samples in every signal period is equal to 6.4 kHz. This gives 128-point FFT at a resolution of 50 Hz. However, at this sampling frequency the transition bandwidth of anti-aliasing filters is only equal to 0.7 kHz. As such, the sampling frequency was increased to 12.8 kHz. This gave a 256-point FFT and transition bandwidth of 3.9 kHz. This solution allows for use of a lower order anti-aliasing filter. 18-bit analogue-to-digital converters were used to acquire the signals in the model.

Results

The results of the simulation tests obtained with signal u_{s1} are presented in Tables 3 and 4 and in Figures 3-10. Due to the limited page count of this article, only a selection of results are given. Figures 3-10 show the frequency characteristics of the half-band filters for the different values of their parameters. Figure 3 shows the amplitude characteristics of the all-pass filters H_{F1} and H_{F2} respectively, for frequencies from 0 Hz to $f_s/2$ Hz. This relates to the filters designed for $d = 1e-2$. These have the identical amplitude characteristics for all the cut-off frequencies f_0 of the Hilbert transformer (Table 1), which were used to calculate the half-band filters.

The characteristics overlap and create one line in these figures. It should be noted that neither of the all-pass filters designed for the other d parameter values had signal amplitude attenuation across the band from 0 Hz to $f_s/2$ Hz.

The following figures present the phase characteristics of the relationship between the transfer functions of the all-pass filters H_{F1}/H_{F2} . This relationship characterises the phase shift between the output signals of the two all-pass filters. Its characteristics should be considered as the phase characteristics of the Hilbert transformer. Figure 4 presents the phase characteristics H_{F1}/H_{F2} for $d = 1e-2$, for the frequency range from 0 Hz to $f_s/2$ Hz. As can be seen, the phase characteristics are sloped, and deflect from -90 degrees at the beginning and end of the frequency band.

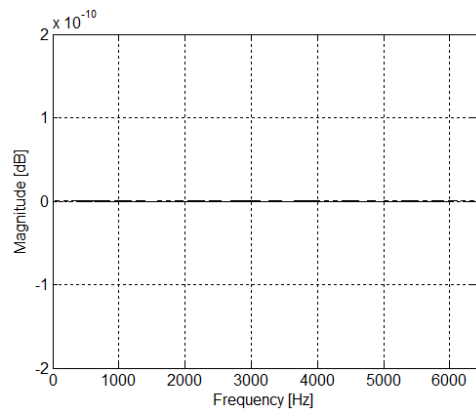


Fig. 3. Magnitude responses of the all-pass filters H_{F1} and H_{F2} for $d = 1e-2$ for frequency range from 0 Hz to $f_s/2$ Hz.

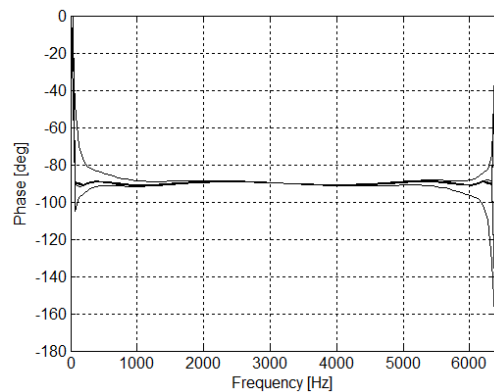


Fig. 4. Phase responses of the half-pass filter H_{F1}/H_{F2} for $d = 1e-2$ for frequency range from 0 Hz to $f_s/2$ Hz.

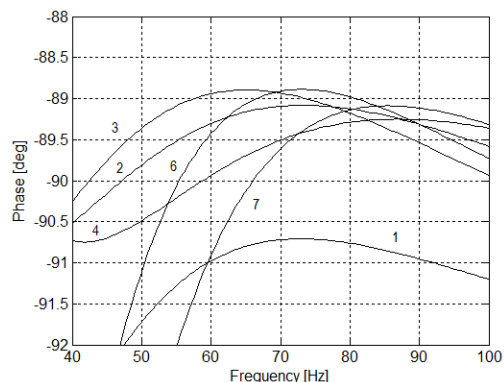


Fig. 5. Phase responses of the half-pass filter H_{F1}/H_{F2} for $d = 1e-2$ for frequency range from 40 Hz to 100 Hz. Where 1 is the characteristic for $f_0 = 5$ Hz, 2 for $f_0 = 10$ Hz, 3 for $f_0 = 20$ Hz, 4 for $f_0 = 30$ Hz, 6 for $f_0 = 50$ Hz, and 7 for $f_0 = 60$ Hz. Characteristics for $f_0 = 40$ Hz (no. 5), and $f_0 = 100$ Hz (no. 8) are out of the scale.

Furthermore, as is shown enlarged in Figure 5 the characteristics have ripples, which introduce a deviation from -90 degrees. The values given in Tables 3 and 4 show that even the smallest deviations in the characteristics of the half-pass filter can cause errors of even several percent in the reactive power measurement. As such, it is important to obtain not only the proper passband of the Hilbert transformer, but also the small ripples in this band, too.

Figure 5 shows that in some cases the characteristics of the half-band filter designed for the small low cut-off frequency f_0 of the Hilbert transformer passband do not pass that close to -90 degrees at 50 Hz frequency. This also applies to filters designed with the use of very small values for ripples d , for which, however, this meant a reduction in the deviation of phase characteristics.

This can be observed in Figures 6-10, which present the phase characteristics of the half-pass filters H_{F1}/H_{F2} with its parameters' different values.

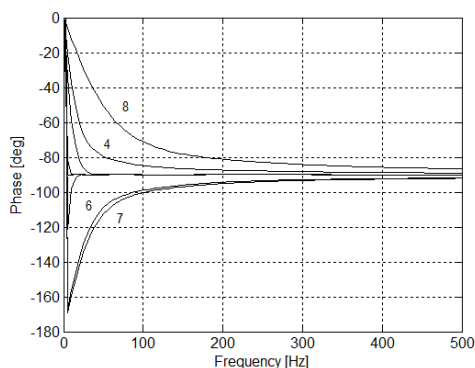


Fig. 6. Phase responses of the half-pass filter H_{F1}/H_{F2} for $d = 1e-3$ for frequency range from 0 Hz to 500 Hz, Where 4 is the characteristic for 30 Hz, 6 for $f_0 = 50$ Hz, 7 for $f_0 = 60$ Hz, and 8 for $f_0 = 100$ Hz.

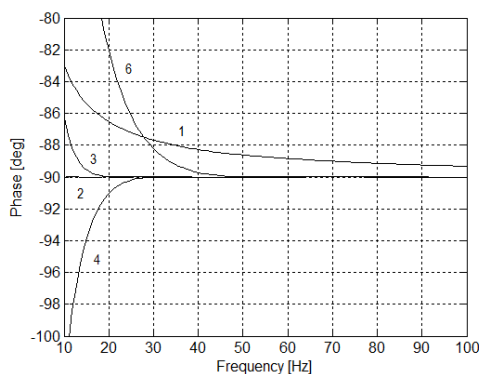


Fig. 7. Phase responses of the half-pass filter H_{F1}/H_{F2} for $d = 1e-4$ for frequency range from 10 Hz to 100 Hz. Where 1 is the characteristic for $f_0 = 5$ Hz, 2 for $f_0 = 10$ Hz, 3 for $f_0 = 20$ Hz, 4 for $f_0 = 30$ Hz, and 6 for $f_0 = 50$ Hz.

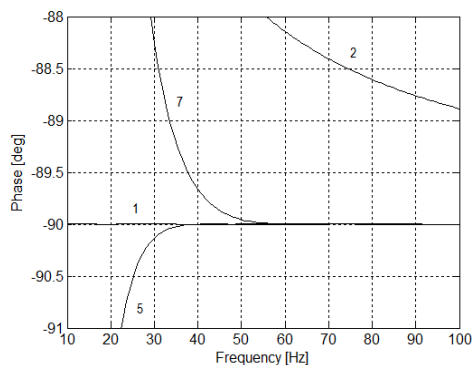


Fig. 8. Phase responses of the half-pass filter H_{F1}/H_{F2} for $d = 1e-5$ for frequency range from 10 Hz to 100 Hz. Where 1 is the characteristic for $f_0 = 5$ Hz, 2 for $f_0 = 10$ Hz, 5 for $f_0 = 40$ Hz, and 7 for $f_0 = 60$ Hz.

The maximum ripples of the phase characteristics meeting the requirements for the width of the passband were, respectively: ± 1.2 deg for $d = 1e-2$ (Fig. 5), ± 0.11 deg for $d = 1e-3$ (Fig. 6), ± 0.011 for $d = 1e-4$ (Fig. 7), ± 0.0012 for $d = 1e-5$ (Fig. 8), ± 0.00012 for $d = 1e-6$ (Fig. 9) and ± 0.000015 for $d = 1e-7$ (Fig. 10).

The results of the measurement error for reactive power calculated using the half-band filters for the various d and f_0 (Tables 3 and 4) showed that a reduction in the value of parameter d did not improve the results of the reactive power measurement for each frequency f_0 , in spite of

reducing the ripples. This problem is because the reduction of d increases the nonlinearity of the phase characteristics of the half-band filters. For example, for $f_0 = 10$ Hz and $d = 1e-5, 1e-6, 1e-7$ (Table 3), the values of the error of the reactive power measurement were amounted to -25%, 21% and -18% in relation to the results obtained from Equation (3).

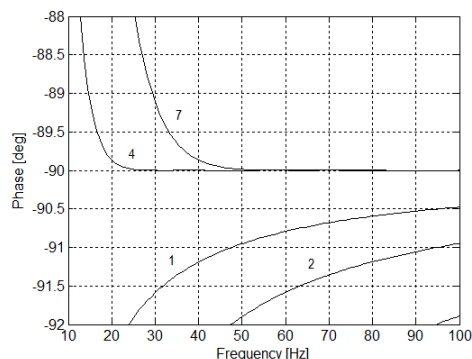


Fig. 9. Phase responses of the half-pass filter H_{F1}/H_{F2} for $d = 1e-6$ for frequency range from 10 Hz to 100 Hz. Where 1 is the characteristic for $f_0 = 5$ Hz, 2 for $f_0 = 10$ Hz, 4 for $f_0 = 30$ Hz, and 7 for $f_0 = 60$ Hz.

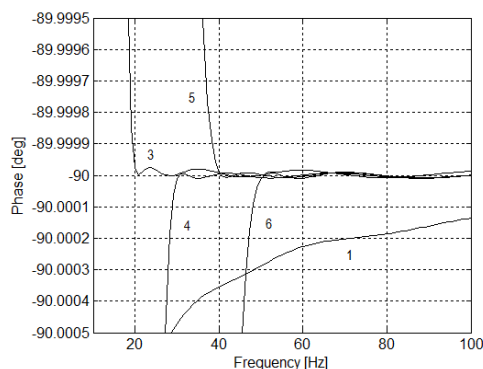


Fig. 10. Phase responses of the half-pass filter H_{F1}/H_{F2} for $d = 1e-7$ for frequency range from 10 Hz to 100 Hz. Where 1 is the characteristic for $f_0 = 5$ Hz, 3 for $f_0 = 20$ Hz, 4 for $f_0 = 30$ Hz, 5 for $f_0 = 40$ Hz and 6 for $f_0 = 50$ Hz.

Table 3. The relative measurement error for $R = 10 \Omega$ and $C = 2$ mF. The results were calculated relative to the value equal to -824.41 Var, obtained from Equation (3).

$f_0 \setminus d$	The relative measurement error [%]					
	$d=1e-2$	$1e-3$	$1e-4$	$1e-5$	$1e-6$	$1e-7$
$f_0 = 5$ Hz	18.97	-0.54	-15.22	0.00	10.44	0.00
10 Hz	-1.98	-0.31	-0.04	-24.51	20.79	-18.20
20 Hz	-6.86	0.07	0.06	-50.06	41.37	0.00
30 Hz	5.39	-116.31	0.07	74.26	0.00	0.00
40 Hz	217.01	0.89	-122.96	0.01	82.57	0.00
50 Hz	12.20	199.41	-0.09	-125.9	-108.66	0.00
60 Hz	39.49	234.55	186.5	-0.47	-0.13	-111.43
100 Hz	-525.97	-421.56	-339.09	-277.44	232.00	-199.11

These results were worse than for $d = 1e-2, 1e-3$ and $1e-4$. Still-worse results for the same frequency f_0 are shown in Table 4. The results obtained for the same filter parameters were absolutely unacceptable. However, for example, the use of $d = 1e-7$ and $f_0 = 20$ Hz given in the two above-quoted cases (Tables 3 and 4) returned measurement error values equal to 0.00 %.

Table 4. The relative measurement error for $R = 10 \Omega$ and $L = 0.1$ mH. The results were calculated relative to the value equal to 17.387 Var, obtained from Equation (3).

The relative measurement error [%]						
$f_0 \backslash d$	$d = 1e-2$	$1e-3$	$1e-4$	$1e-5$	$1e-6$	$1e-7$
$f_0 = 5$ Hz	-924	26,44	738	0,10	-508	-0,16
10 Hz	96.0	15,24	2,18	1187	-1013	882
20 Hz	333	-3,53	-2,88	2417	-2022	0.00
30 Hz	-262	5570	-3,39	-3645	-0,05	-0,01
40 Hz	-10872	-43.0	5884	-0,32	-4057	0.00
50 Hz	-593	-9963	4,60	6022	5209	-0,01
60 Hz	-1929	-11784	-9296	22,97	6,46	5340
100 Hz	23732	19369	15772	13014	109	9437

Similar comparisons can be found for the other frequencies f_0 and d . It should also be noted that in some cases the values of the error were extremely great, which eliminated the possibility of using certain sets of parameters.

Comparative analysis of the phase characteristics of all the Hilbert transformers made with the use of the half-band filters and the obtained results (Figs. 3-10, Tables 3 and 4) indicated that the smallest error values were obtained using half-band filters with the following parameters: $f_0 = 5.2$ Hz and $d = 1e-5$ as well as $f_0 = 20$ Hz, 30 Hz, 40 Hz, 50 Hz and $d = 1e-7$. It should be noted that when $d = 1e-7$ the filters for $f_0 = 5$ Hz and 10 Hz did not meet the established accuracy criterion, although they did give the widest passband in the transformer. However, the criterion was met by the half-band filter with a lower cut-off frequency f_0 of 50 Hz, which is the first harmonic. This confirmed the thesis that when designing the Hilbert transformer using the half-band filter, consideration should be given to the lowest frequency f_0 as this can lead to the large measurement errors, even at very small d .

The five selected filters were also tested using signal u_{s2} . All five enabled measurement of reactive power with the maximum relative error $\pm 0.01\%$ at all of the tested loads, and for both test signals, u_{s1} and u_{s2} , at the sampling frequency of 12.8 kHz. In order to arrive at the most accurate instrument, a maximum measurement error was assumed equal to $\pm 0.01\%$.

The selected filters were also tested with other sampling frequencies, equal to 10 kHz, 5 kHz, and 2.5 kHz. In all cases, the obtained results for reactive power bore comparison with the results obtained with the sampling frequency equal to 12.8 kHz, and with the results obtained from (3). Only four filters, for $f_0 = 20$ Hz, 30 Hz, 40 Hz, 50 Hz and $d = 1e-7$, passed all tests. Of the four half-band filters which met the accuracy criterion, the best filter – in terms of the number of coefficients of all-pass filters – was the half-band filter designed for the frequency $f_0 = 40$ Hz and $d = 1e-7$. The coefficients for this filter are given in Table 5.

Table 5. Coefficients of the half-band filter with parameters $f_0 = 40$ Hz and $d = 1e-7$.

i - index of the coefficient a_i	Values of the coefficients of the all-pass filter H_{F1}	Values of the coefficients of the all-pass filter H_{F2}
0	12.77682203135281	0.02037133289752
1	3.71324473529900	0.16506481726003
2	2.05507244449140	0.37957308924292
3	1.49447541819616	0.58419407116651
4	1.25162489260591	0.74051173143580
5	1.13219541570260	0.84593926035847
6	1.06842199472485	0.91268434039588
7	1.03118313540206	0.95455527596383
8	1.00567856751073	0.98269299296319

Conclusions

In this paper, a comparative analysis of Hilbert transformers built using 50 half-band filters with different parameters has been made. The author's tests have shown that small changes in the values of the filter parameters have a significant influence on the accuracy of signal shifts, and consequently on the accuracy of reactive power measurement. Furthermore, in spite of reducing ripples, decrease of the values of parameter d did not always improve measurement results. The same is true of frequency f_0 – its reduction did not always cause an increase in the accuracy of reactive power measurement. Comparative analysis of the filters' characteristics and the reactive power measurement results helped to determine the best half-band filter, for which the obtained values of the relative error of the reactive power measurement were less than or equal to 0.01% for all considered types of load parameters, signals and sampling frequencies. This filter was designed for the frequency $f_0 = 40$ Hz and $d = 1e-7$. It should be noted that it had better properties than the filters designed for lower f_0 frequencies.

REFERENCES

- [1] Lyons, R., Understanding digital signal processing, Prentice Hall, (2004).
- [2] Zieliński, T. P., Digital signal processing. From theory to practice, Wydawnictwa Komunikacji i Łączności, (2009).
- [3] Nowomiejski, Z., Generalized theory of electrical power, Archiw fur Elektrotechnik, 59, (1977), 183-189.
- [4] Pasko, M., Power theory review for systems with distorted signals, Proc. of EPN-2002, Poland, Zielona Góra, (2002), 11-46.
- [5] Budeanu, C.I., Puissance reactiva et fictives, RGE, T.XXIII, (1928), 762-773.
- [6] Iliovici M., Definition et mesure de la puissance et de lenergie reactiva, Bull. Soc. Franc. Electr., 5, (1925), 931-954.
- [7] IEEE Std 1459-2010: Standard Definitions for the Measurement of Electric Power Quantities Under Sinusoidal, Nonsinusoidal, Balanced, or Unbalanced Conditions, (2010).
- [8] Papierz, K., Reactive power measurement using Hilbert transformation in according with IEEE Std 1459-2010, Informatyka, Automatyka, Pomiar w Gospodarce i Ochronie Srodowiska, 4, (2011) 15-18.
- [9] Oppenheim, A.A., and Schaffer, R.W., Digital signal processing, Prentice-Hall, Inc., (1975).
- [10] Pang, H., Wang, Z., and Chen, J., A measuring method of the single-phase ac frequency, phase, and reactive power based on the Hilbert filtering, IEEE Transactions on Instrumentation and Measurement, 56, no. 3, (2007), 918-923.
- [11] Johansson H., and Wanhammar L., Digital Hilbert transformers composed of identical allpass subfilters, Proceedings of the 1998 IEEE International Symposium on Circuits and Systems, USA, Monterey, CA, 5: (1998), 437-440.
- [12] Ansari, R., Elliptic filter design for a class of generalized halfband filters, IEEE Transactions on Acoustics, Speech and Signal Processing, 33, (1985), no. 5, 1146-1150.
- [13] Ansari, R., IIR discrete-time Hilbert transformers, IEEE Transactions on Acoustics, Speech and Signal Processing, 35, (1987), no. 8, 1116-1119.
- [14] Jackson L., Digital filters and signal processing. Third edition with Matlab exercises, Kluwer Academic Publishers, (1996).
- [15] Pun, KP., da Franca, JE., and Azeredo-Leme, C., Circuit design for wireless communications. Improved Techniques for Image Rejection in Wideband Quadrature Receivers, Springer-science+business media, b.v., (2003).
- [16] Schussler, H.W., and Steffen, P., Halfband filters and Hilbert transformers, Circuits Systems Signal Processing, 17, (1998), no. 2, 137-164.

Author: dr inż. Adam Graczyk, Politechnika Łódzka, Wydział Elektrotechniki, Elektroniki, Informatyki i Automatyki, Instytut Systemów Inżynierii Elektrycznej, ul. B. Stefanowskiego 18/22, 90-924 Łódź, e-mail: agraczyk@p.lodz.pl